

Single-molecule imaging of protein adsorption mechanisms onto surfaces

Shannon Kian Zareh and Y. M. Wang

Department of Physics, Washington University in St. Louis, St. Louis, MO, 63130

Mailing address: 244 Compton Hall, 1 Brookings Dr., St. Louis, MO, 63130

Corresponding author: Y. M. Wang; Address: 244 Compton Hall, 1 Brookings Dr., St. Louis, MO, 63130

Office phone: 314-935-7478

Keywords: Single-protein adsorption detection, irreversible and reversible protein adsorption kinetics

Abstract

Protein-surface interactions cause the desirable effect of controlled protein adsorption onto biodevices as well as the undesirable effect of protein fouling. The key to controlling protein-surface adsorptions is to identify and quantify the main adsorption mechanisms: adsorptions that occur (1) while depositing a protein solution onto dry surfaces and (2) after the deposition. Bulk measurements cannot reveal the dynamic protein adsorption pathways and thus cannot differentiate the two adsorption mechanisms. We have performed real-time single-molecule imaging experiments of streptavidin adsorption to hydrophobic fused-silica surfaces. We have observed both adsorbed proteins on surfaces and diffusing proteins near surfaces and analyzed their adsorption kinetics. Our analysis indicates that the deposition process is the primary cause of protein adsorption onto surfaces for sub-nanomolar to nanomolar protein concentrations. We have also observed that hydrophilic fused-silica surfaces prevent the adsorption of streptavidin proteins.

INTRODUCTION

Controlled surface adsorption of proteins is important for devices such as protein-based biosensors and protein microarrays; on the other hand, uncontrolled accumulation of proteins on surfaces causes undesirable protein fouling (Zydny and Ho, 2003). In addition, when protein-surface contact is involved in a process, controlling protein-surface adsorption is necessary to ensure minimal perturbation to protein concentration and characteristics in solution. For these reasons, it is necessary to identify and quantify mechanisms responsible for protein binding to surfaces.

The first step in most protein-based biological studies and applications involves introducing a protein solution to a device (e.g., pipette tip, transfer tube, glass slide, etc.). It is known that proteins can dissolve in water as well as accumulate on water surfaces at the water-air interface (Mackie et al., 1999; de Jongh et al., 2004; Deng et al., 2006; Yano et al., 2009). When these proteins encounter a device surface, some may adsorb during the protein-solution deposition process while others may adsorb after the surface is wet. These adsorptions are the result of electrostatic, van der Waals, and hydration interactions between proteins and surfaces (Squires et al., 2008).

Most studies focus on surface adsorptions of the dissolved proteins after deposition (Vasina et al., 2009), and the effects of the deposition process have not been considered.

In order to precisely identify and quantify mechanisms responsible for protein-surface adsorptions, it is necessary to image the adsorption process of individual proteins. Prior studies on protein-surface interactions have mainly used bulk ensemble measurements, in which the total concentrations of all adsorbed proteins were measured and thus adsorptions due to different mechanisms could not be differentiated (Sapsford and Ligler, 2004; Tsapikouni and Missirlis, 2008). To address this issue, we used Total Internal Reflection Fluorescence (TIRF) microscopy imaging to record the interaction of single streptavidin-Cy3 (and streptavidin-Alexa555) molecules with hydrophobic and hydrophilic fused-silica surfaces in real time. Images of both adsorbed proteins at the surfaces and free 3D-diffusing proteins near the surfaces were captured to reveal the adsorption pathways and kinetics for both mechanisms.

MATERIALS AND METHODS

Protein Deposition

Figures 1 (A) – (C) illustrate the streptavidin protein-solution deposition method onto fused-silica surfaces (6W675-575 20C, Hoya Corporation USA, San Jose, CA). Five microliters of streptavidin-Cy3 powder (SA1010, Invitrogen, Carlsbad, CA) or streptavidin-Alexa555 powder (S21381, Invitrogen, Eugene, OR) dissolved in 0.5 X TBE solution (pH = 8) to 0.3 nM concentration were deposited onto a fused-silica surface by pipette. Streptavidin is a 52.8-kDa tetrameric protein measuring $4.5 \times 4.5 \times 5$ nm in size (Scouten and Knechty, 1992). It has an isoelectric point of 6.3 (Sivasankar et al., 1998) and is negatively charged in pH 8 solutions. Protein concentrations of less than nanomolars were used such that images of individual adsorbed proteins on surface and 3D-diffusing proteins in solution could be resolved without overlapping. A coverslip flattened the droplet for imaging. Using this protein-solution deposition method, both protein adsorption mechanisms are present: the initial protein-surface interactions during the deposition process onto dry fused-silica surfaces and the later protein-surface interactions after the deposition. Since hydrophobic surfaces are known to yield higher protein-surface adsorption affinity than hydrophilic surfaces (Israelachvili, 1992), the surfaces in Figs. 2, 3, and 4 (A) were treated to be hydrophobic with a $\approx 90^\circ$ water contact angle by dipping oxygen-plasma-cleaned fused-silica chips into a 5% dichlorodimethylsilane in chloroform solution for 10 sec. The glass coverslip was cleaned using oxygen plasma and was hydrophilic. After protein deposition, the coverslip edges were sealed with nail polish.

Imaging Setup

Single-molecule imaging was performed using a Nikon Eclipse TE2000-S inverted microscope (Nikon, Melville, NY) in combination with a Nikon 100X objective (Nikon, 1.49 *N.A.*, oil immersion). Samples were excited by prism-type TIRF microscopy with a linearly polarized 532 nm laser line (I70C-SPECTRUM Argon/Krypton laser, Coherent Inc., Santa Clara, CA) focused to a $40 \mu\text{m} \times 20 \mu\text{m}$ region. The laser excitation was pulsed with illumination intervals of 0.3 ms to 28 ms, and the durations between images were one hour for Figs. 2 and 3, and 30 ms for Figs. 4 and 5. The excitation intensities were $0.3 \text{ kW/cm}^2 - 8 \text{ kW/cm}^2$. Images were captured by an iXon back-illuminated electron multiplying charge coupled device (EMCCD) camera (DV897ECS-BV,

Andor Technology, Belfast, Northern Ireland). An additional 2X expansion lens was placed before the EMCCD, producing a pixel size of 79 nm. The excitation filter was 530 nm/10 nm and the emission filter was 580 nm/60 nm.

Data Analysis

Typical movies were obtained by synchronizing the onset of camera exposure with laser illumination. The gain levels of the camera were adjusted such that none of the pixels of a single molecule’s point spread function (PSF) reached the saturation level of the camera. For a selected image, the intensity values of 20×20 pixels centered at the molecule were recorded. One dimensional intensity profile of the molecule was obtained by averaging the 20 transverse pixel values at each of the 20 horizontal pixels. The 1D intensity profiles were then fitted to a 1D Gaussian function using a least squares curve-fitting algorithm (lsqcurvefit) provided by MATLAB (The Mathworks, Natick, MA):

$$f(x) = f_0 \exp\left(-\frac{(x - x_0)^2}{2s^2}\right) + \langle b \rangle, \quad (1)$$

where f_0 is the amplitude, x_0 is the center, $\langle b \rangle$ is the mean background value, and s is the standard deviation (SD) of the molecule’s intensity profile. Using the SD value of a single molecule intensity profile, we determined whether the molecule was adsorbed on the surface or diffusing in the solution (see Results below).

RESULTS

Figure 2 shows a time series of streptavidin-Alexa555 images on a hydrophobic fused-silica surface separated by 4 minutes, starting right after deposition. The diffraction-limited dots and the larger “blurs” of images are adsorbed and diffusing proteins on the surface and in the solution, respectively. The long intervals of minutes between the images were chosen to minimize fluorophore bleaching due to frequent illumination (Wang et al., 2005) and to demonstrate the binding of irreversibly adsorbed proteins. In order to determine whether a fluorescent image is a stationary protein on the surface or a diffusing protein in solution, we measured the SD of the the molecule’s fluorescence intensity profile (Wang et al., 2005; Wang et al., 2006). If the SD value was within the diffraction limit of the imaging system ($\approx 120 \pm 20$ nm), the molecule was adsorbed on the surface (DeSantis et al., 2010; DeCenzo et al., 2010); if the SD was larger than 140 nm, it was a diffusing protein.

The molecules with SD values below 140 nm that didn’t change location in all four images are denoted by yellow slanted arrows. Since there was no location change for these proteins after the deposition, they are irreversibly adsorbed proteins. Also, since there were no additional irreversibly adsorbed proteins after the deposition, these proteins must have been adsorbed during the protein-solution deposition process. The molecules with SD values below 140 nm and that only appeared in one image are denoted by green vertical arrows. These are reversibly bound proteins adsorbed after the deposition with dissociation time shorter than 4 minutes (real dissociation time is discussed below). The blurred molecules with SD larger than 140 nm, and that also only appeared in one image are 3D diffusing proteins and are denoted by red horizontal arrows.

In order to demonstrate that (1) the irreversibly adsorbed proteins remain at the same locations for a long time after the sample deposition, and (2) the reversibly adsorbed proteins and (3) the 3D-diffusing proteins change locations from image to image, in Fig. 3 we superpositioned two

images taken at two different times: immediately after the deposition (proteins are false-colored red), and 38 minutes after the deposition (proteins are false-colored green). Each image contains both adsorbed proteins on the surface and 3D-diffusing proteins near the surface. We chose the superposition of false-green proteins in image 1 and false-red proteins in image 2 to be represented by orange dots.

The orange proteins were on the surface right after the deposition and did not dissociate in 38 minutes. In one experiment we observed irreversibly adsorbed proteins over one night, indicating that the proteins are indeed irreversibly adsorbed. The small green and red dots in Fig. 3 are proteins that are reversibly adsorbed on the surface after the deposition. Note that the reversibly bound proteins in Figs. 2 and 3 were at different locations for the two different imaging times separated longer than the dissociation time of the reversibly adsorbed proteins. This observation is consistent with reversible adsorption kinetics, in which the same number of proteins are adsorbed at random locations on the surface when at equilibrium.

To study the kinetics of these reversible adsorptions, a faster frame imaging rate was used: 33 Hz imaging rate and 28 ms exposure time. Figure 4 (A) shows montage of images of a molecule diffusing towards a surface, binding to, and dissociating from it. Going from top to bottom of the montage, the large blurs in images 2 and 8 of the montage are the incoming molecule moving towards the surface, and the outgoing molecule leaving the surface, respectively. The dissociation time of this molecule is ≈ 140 ms (5 frames). The binding times of ≈ 200 reversibly bound proteins were measured and the mean reversible binding time of streptavidin to dichlorodimethylsilane hydrophobic surfaces was ≈ 200 ms (6 imaging frames of 28 ms each).

In order to verify that the large blurred images in Figs. 2, 3, and 4 with SD larger than 140 nm are 3D-diffusing molecules, we studied how the SDs of these molecules change with exposure time. If they were 3D-diffusing molecules, SD should increase with exposure time since SD is a reflection of how far a molecule diffuses during exposure. The penetration depth of TIRF evanescent light is ≈ 150 nanometers, so for this study we chose short exposure times such that proteins would not diffuse beyond twice the penetration depth for complete capture of the 3D-diffusing molecule diffusion pathway. With the Brownian dynamics calculation of $\langle x^2 \rangle = 2D_3t$, where $\langle x^2 \rangle$ is the mean square displacement of 3D-diffusing molecules, $D_3 \approx 5 \times 10^7 \text{ nm}^2/\text{s}$ is the 3D-diffusion coefficient for streptavidin with ≈ 5 nm diameter, and t is the exposure time, the appropriate exposure time t should be in the sub-millisecond range such that $\langle x^2 \rangle$ is less than 300 nanometers.

Figures 5 (A), (B), and (C) show representative 3D-diffusing molecules with increasing exposure times of 0.3 ms, 0.7 ms, and 1 ms, respectively. It is obvious that the width of the molecule increases with exposure time. Figure 5 (D) shows the SD distributions for the three exposure times, and the mean SD values are larger than ≈ 140 nm, and increase with exposure time. This observation proves that the observed molecules with SD larger than 140 nm are indeed 3D-diffusing streptavidin-Cy3 molecules near the surface.

We calculated the fractions of adsorptions occurred during and after the deposition process by analyzing the adsorption statistics for Fig. 3. Of all the proteins in Fig. 3, 32 molecules were irreversibly adsorbed by the deposition-induced binding mechanism (orange); 2 were reversibly adsorbed by protein-surface interactions at the water-surface interface (green or red); and about 30 were 3D-diffusing proteins not adsorbed at the time of the imaging (green or red). These results show that at the molecular concentration of 0.3 nM, the main cause of streptavidin-surface adsorption is the protein-deposition process, which accounts for $32/(32+2=34) \approx 94\%$ of the total

surface-adsorbed proteins at all times. The protein-surface interactions after the deposition are responsible for only $2/34 \approx 6\%$ of the total adsorption. The majority of 3D-diffusing proteins near surfaces do not bind to the surfaces: only $\approx 2/(30/\text{frame} \times 6 \text{ frames} = 180) \approx 1\%$ proteins that encounter the surface reversibly bind to it. Figure 2 shows similar adsorption statistics for the same concentration of streptavidin. We have measured various increasing streptavidin concentrations to 5 nM (at which individual molecule images begin to overlap) and observed that such deposition-induced adsorptions dominate for streptavidin interaction with hydrophobic fused-silica surfaces.

The above results show that even for a “sticky” hydrophobic surface, the dominating mechanism responsible for streptavidin fused-silica surface adsorption at sub-nanomolar and nanomolar concentrations is the deposition process. For hydrophilic surfaces that are believed to be less “sticky” to some proteins, how does the protein-surface adsorption change? The fused-silica chip was made hydrophilic by performing oxygen plasma cleaning for 2 minutes. We observed complete elimination of irreversible and reversible streptavidin-surface adsorption on hydrophilic fused-silica surfaces for the observation time of at least hours. Figure 4 (B) shows that there are only 3D-diffusion proteins near the hydrophilic surface and no adsorbed proteins. This result indicates that hydrophilic surfaces prevent streptavidin fouling of surfaces.

DISCUSSION

Deposition-process-associated irreversible adsorptions

What is the possible mechanism that causes the irreversible protein adsorptions during deposition? If we assume that the surface is chemically stable from the moment water touches the surface, a dissolved protein’s interaction with the surface at the water-surface interface has the same affinity during the deposition as after the deposition. However, during the deposition process, air is an additional component in the protein-surface interface—and this may result may result in a different protein-surface binding affinity and consequently, irreversible adsorption for most proteins at the air-water interface.

To investigate the ratio of surface-protein concentration to bulk protein concentration, we have observed the surface proteins by imaging the edges of a protein droplet on glass (using the method described by Deng et al., 2006) and determined the concentrations to be comparable. This observation agrees with our result that 32 of the total 64 proteins imaged in one snapshot are irreversibly adsorbed on the surface, indicating comparable air-water interface protein concentration to the bulk protein concentration.

Reversible adsorptions

The adsorptions that occurred after the deposition are caused by genuine interaction of streptavidin amino-acids with surface chemical groups. These interactions include hydrophobic, ionic, and van der Waals interactions (Sequires et al., 2008; Heinz et al., 2009). The net charge of streptavidin is negative in pH 8 buffer, and it is hydrophilic (van Oss et al., 2003). The fused-silica surface groups are dimethylsilane groups and silanol groups for the hydrophobic and hydrophilic surfaces, respectively. Our observed reversible binding for hydrophobic surfaces indicates that the net binding affinity between streptavidin and the surface groups is strong enough for reversible binding to occur on hydrophobic surfaces, but not strong enough for binding to occur on hydrophilic surfaces.

Other hydrophobic surfaces and proteins

To determine the role hydrophobicity plays in streptavidin-surface adsorptions, we have investigated streptavidin interaction with three differently treated hydrophobic surfaces: RainX (SOPUS Products, Houston, TX), lab detergent (Versa-Clean, 04-342, Fisher Scientific, Pittsburgh, PA), and 0.1 wt% solution of dodecyltrichlorosilane in hexane. The adsorption results are the same as for the dichlorodimethylsilane treated surfaces: we have observed both irreversible and reversible adsorptions, with the irreversible adsorptions outnumbering the reversible adsorptions. We have also changed the degree of hydrophobicity by changing the ratio of dichlorodimethylsilane to chloroform and thus the contact angles from approximately 30° to 90°. We observed less irreversible and reversible adsorptions with decreasing hydrophobicity. These observations indicate that hydrophobic interactions dictate interactions between streptavidin and hydrophobic fused-silica surfaces. We have also studied surface adsorptions using green fluorescent proteins and Lactose repressor proteins with similar results observed.

Competition for surface binding between protein and water molecules

In addition to proteins, water molecules also have affinity for binding to surfaces. Water competes with streptavidin for surface binding. This competition may also contribute to the observed streptavidin adsorptions.

In Figs. 1 (D) and (E) we show possible competitions between a protein with water molecules for binding to hydrophobic and hydrophilic surfaces, respectively. Streptavidin is hydrophilic, but less so than water. So when encountering a hydrophobic surface, water avoids the surface more than streptavidin, leading to an effective increased protein exposure to the surface, and consequently increased adsorptions (Fig. 1D). For the hydrophilic surface, water molecules are attracted to the surface more than streptavidin, leading to decreased streptavidin adsorption to surface (Fig. 1E).

Deposition variations

Variations to procedures in transferring proteins to devices include changing the fluid flow speed, and transferring proteins to wet surfaces. We have varied the pipetting speed when depositing proteins onto dry hydrophobic and hydrophilic surfaces, varying the fluid flow speed by at least 10-fold, and have observed no difference in irreversible and reversible adsorption characteristics. We have also transferred protein solutions to a wet surface, and imaged in real time. We observed only diffusing proteins in solution and reversible adsorptions. This result indicates the importance of the air interface in protein-surface irreversible adsorptions.

CONCLUSION

In summary, single-molecule real-time imaging of protein-surface interactions provides a tool to differentiate among adsorption mechanisms and kinetics. We have shown that protein-surface irreversible and reversible adsorptions are highly process dependent at sub-nanomolar and nanomolar concentrations. These results indicate that in addition to regulating post-deposition protein-surface interactions, the deposition-process must be taken into consideration in the design and interpretation of protein-surface adsorption studies. The observation that surface adsorption of streptavidin can be avoided with hydrophilic surfaces may have important implications for prevention of protein fouling in general.

References

- DeCenzo SH, DeSantis MC, Wang YM. 2010. Single-image separation measurements of two unresolved fluorophores. *Opt Express* 18(16):16628-16639.
- de Jongh HHJ, Kosters HA, Kudryashova E, Meinders MBJ, Trofimova D, Wierenga PA, 2004. Protein Adsorption at Air-Water Interfaces: A Combination of Details. *Biopolymers* 74:131135.
- Deng Y, Zhu YY, Kienlen T, Guo A. 2006. Transport at the air/water interface is the reason for rings in proteins microarrays. *J AM Chem Soc Comm* 128:27682769.
- DeSantis MC, DeCenzo SH, Li JL, Wang YM. 2010. Precision analysis for standard deviation measurements of immobile single fluorescent molecule images. *Opt Express* 18(6):6563-6576.
- Gray JJ. 2004. The interaction of proteins with solid surfaces. *Curr Opin Struct Biol* 14:110115.
- Heinz H, Farmer BL, Pandey RB, Slocik JM, Patnaik SS, Pachter R, Naik RR, 2009. Nature of Molecular Interactions of Peptides with Gold, Palladium, and Pd-Au Bimetal Surfaces in Aqueous Solution. *J Am Chem Soc* 131:97049714.
- Israelachvili JN. 1992. Intermolecular and surface forces. 2nd edn. Academic Press.
- Latour RA. 2005. Biomaterials: Protein-Surface Interactions. New York: Taylor & Francis. 1p.
- Mackie AR, Gunning AP, Wilde PJ, Morris VJ, 1999. Orogenic Displacement of Protein from the Air/Water Interface by Competitive Adsorption. *J Colloid Interface Sci* 210:157166.
- Sapsford KE, Ligler FS. 2004. Real-time analysis of protein adsorption to a variety of thin films. *Biosens and Bioelectron* 19:10451055.
- Sivasankar S, Subramaniam S, Leckband D, 1998. Direct molecular level measurements of the electrostatic properties of a protein surface. *Proc Natl Acad Sci* 95:1296112966.
- Squires TM, Messinger RJ, Manalis SR. 2008. Making it stick: convection, reaction and diffusion in surface-based biosensors. *Nat Biotechnol* 26(4):417426.
- Tsapikouni TS, Missirlis YF. 2008. Protein-material interactions: From micro-to-nano scale. *Mater Sci Eng B* 152:27.
- Vasina EN, Paszek E, Nicolau DV, Nicolau DV. 2009. The BAD project: data mining, database and prediction of protein adsorption on surfaces. *Lab Chip* 9:891 900.
- van Oss CJ, Giese RF, Bronson PM, Docoslis A, Edwards P, Ruyechan WT, 2003. Macroscopic-scale surface properties of streptavidin and their influence on aspecific interactions between streptavidin and dissolved biopolymers. *Colloids Surf., B* 30:25 36.

Wang YM, Austin RH, Cox EC. 2006. Single molecule measurements of repressor protein 1D diffusion on DNA. *Phys Rev Lett* 97:048 302.

Wang YM, Tegenfeldt J, Reisner W, Riehn R, Guan XJ, Guo L, Golding I, Cox EC, Sturm J, Austin RH. 2005. Single-molecule studies of repressor-DNA interactions show long-range interactions. *Proc Nat Acad Sci USA* 102:97969801.

Yano YF, Uruga T, Tanida H, Toyokawa H, Terada Y, Takagaki M, Yamada H, 2009. Driving Force Behind Adsorption-Induced Protein Unfolding: A Time-Resolved X-ray Reflectivity Study on Lysozyme Adsorbed at an Air/Water Interface. *Langmuir* 25:3235.

Figure Legends

Figure 1. (A) – (C) Schematic of the protein (orange) deposition process. (D) and (E), protein and water (blue) competing for binding to hydrophobic and hydrophilic surfaces, respectively.

Figure 2. (A) – (D), time series of streptavidin-Alexa555 adsorbed on and diffusing near a hydrophobic fused-silica surface. The first image was acquired right after the deposition, and other images were 4 minutes apart. Yellow slanted arrows indicate irreversibly bound proteins due to the deposition process (in B); green vertical arrows indicate reversibly bound proteins after the deposition (A – D); and red horizontal arrows indicate 3D-diffusing proteins (A – D). The scale bar is 1 μm .

Figure 3. Superposed TIRF images of the streptavidin-Cy3 molecules immediately after deposition (false-colored red) and 38 minutes after the deposition (false-colored green). When the images overlap, the red and green dots yield orange dots (denoted by orange solid arrows). The single-colored red and green molecules with SD less than 140 nm (solid green and red arrows) are reversibly adsorbed proteins after the deposition. The large green and red blurs are 3D-diffusing molecules near the surface (dashed red and green arrows). The scale bar is 1 μm .

Figure 4. (A) Montage of a reversibly bound molecule diffusing towards, binding to, and dissociating from the surface, respectively from top to bottom. (B) 3D-diffusing proteins near a fused-silica hydrophilic surface. Note that there are no adsorbed proteins on the surface. Scale bars are 1 μm .

Figure 5. Images of representative single 3D-diffusing molecules with exposure times of (A) 0.3 ms, (B) 0.7 ms, and (C) 1 ms. The width of the molecules increases with exposure time and the 1D fit SD values are 135 nm (A), 180 nm (B), and 204 nm (C), respectively. (D) SD distribution of the diffusing molecules' intensity profiles for exposure times of 0.3 ms (red), 0.7 ms (blue), and 1 ms (yellow). The SD values are 139.5 ± 3.6 nm (mean \pm standard error of the mean), 173.3 ± 4.2 nm, and 194.5 ± 5.2 nm, respectively. The scale bar is 1 μm .

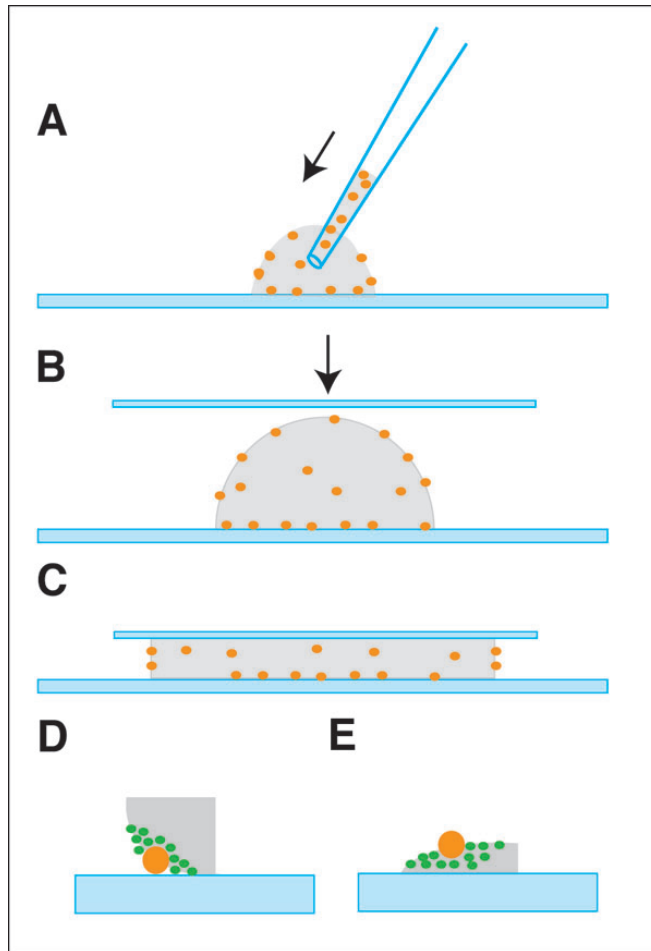


Figure 1:

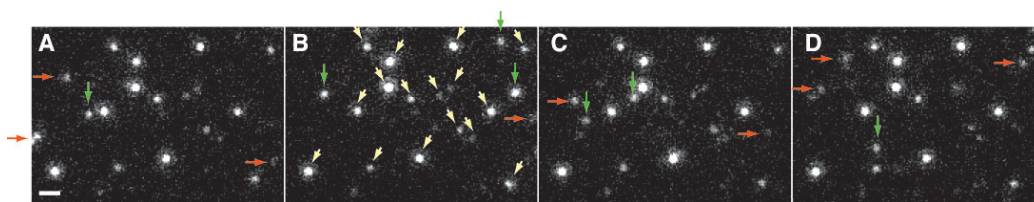


Figure 2:

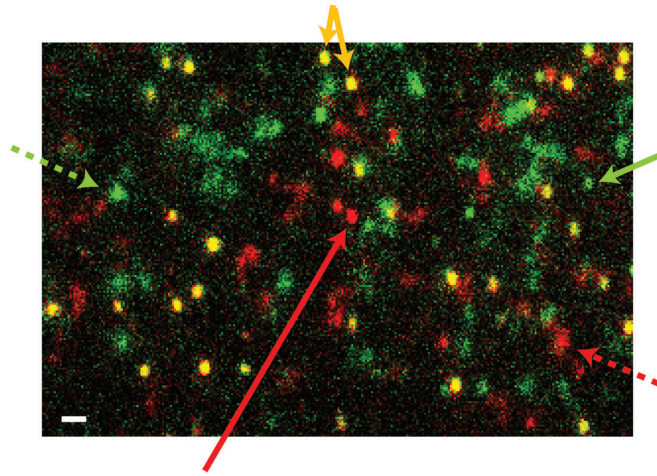


Figure 3:

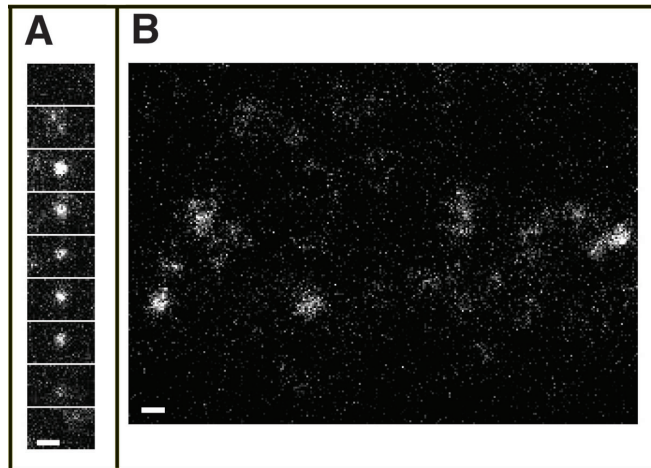


Figure 4:

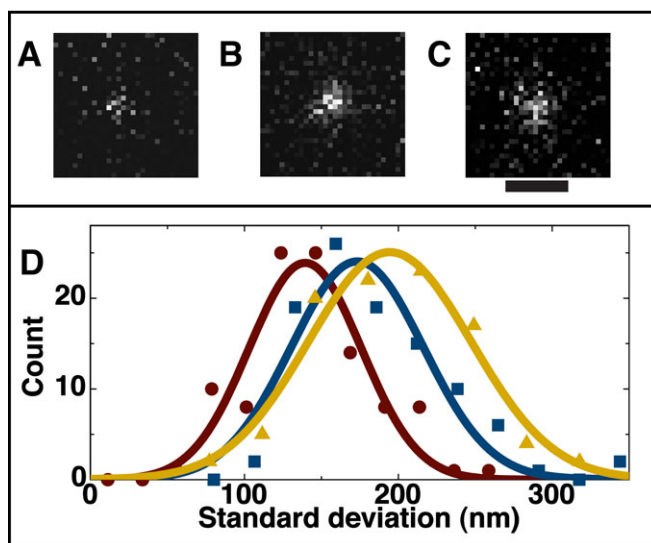


Figure 5: